J Control Autom Electr Syst (2013) 24:397–408
DOI 10.1007/s40313-013-0052-z

A Robust Adaptive Path-Following Controller for a Robotic Wheelchair

Wanderley Cardoso Celeste · Teodiano Freire Bastos-Filho · Mario Sarcinelli-Filho · Celso De La Cruz · Ricardo Carelli

Received: 24 February 2012 / Revised: 9 July 2012 / Accepted: 14 November 2012 / Published online: 8 June 2013

Abstract This article proposes a path-following controller for robotic wheelchairs (RW) used to transport people suffering of severe muscular diseases, taking into account velocity bounds and dynamic effects. A parameterized dynamic model, which considers the person on board the RW, is used. The model parameters normally change, generating structured uncertainties. Moreover, the dynamic model is proposed under some simplifications, introducing unstructured uncertainties. Finally, time-varying dynamics, caused basically by user movements, are also considered. Hence, the dynamic controller proposed is adaptive and robust. Experimental and simulation results show the effectiveness and the good performance of the proposed control system.

Keywords Robotic wheelchair · Path following · Dynamic effects · Dynamic uncertainties · Robust adaptive control

W. C. Celeste (✉)
Department of Computing and Electronics, Federal University of Espirito Santo, São Mateus, Brazil
e-mail: cawander@gmail.com; wanderley.celeste@ufes.br

T. F. Bastos-Filho · M. Sarcinelli-Filho · C. De La Cruz
Department of Electrical Engineering, Federal University of Espirito Santo, Vitória, Brazil
e-mail: tfbastos@ele.ufes.br

M. Sarcinelli-Filho
e-mail: sarcinel@ele.ufes.br

C. De La Cruz
e-mail: celsodelacruz@gmail.com

R. Carelli
Institute of Automatics of the National University of San Juan, San Juan, Argentina
e-mail: rcareli@inaut.edu.ar

1 Introduction

Mobile robotics have been widely adopted as augmentative systems in the last decade, allowing one to improve the mobility of people suffering from severe muscular diseases. Robotic wheelchairs (RWs) (Kim et al. 2004; Parikh et al. 2007) associated with human–machine interfaces based on eye movement or brain signals for command selection have been increasingly adopted. This is the case of the experimental platform used in this study, shown in Fig. 1.

RWs introduce important dynamic issues, because they transport a person who represents a heavy and mobile load. A parameterized dynamic model of a RW with a mobile load was proposed in Cruz et al. (2011a) and used to adaptive positioning and trajectory-tracking control. Results of experiments with a RW prototype allow for a positive evaluation of the proposed model.

From these results, one can notice that an adaptive controller is useful because the dynamic parameters normally change after a long-term because of load changes of the vehicle, introducing structured uncertainties (Patre et al. 2008; Aström and Wittenmark 2008). Moreover, model simplifications introduce unstructured uncertainties (Patre et al. 2008), although some disturbance sources, such as sliding velocities and external forces, can be analytically foreseen as non-identifiable but clearly bounded parameters. That is a fundamental issue for obtaining robust adaptive control systems through well-known techniques such as feedback linearization (Isidori 1989), fuzzy sliding mode (Bessa and BarrOto 2010) and backstepping procedure (Fierro and Lewis 1997; Tanner and Kyriakopoulos 2003).

Time-varying dynamics [very common in underwater vehicles (Jordan and Bustamante 2008), for instance] are normally not taken into account when dealing with terrestrial vehicles. In general, such dynamics changes are slow

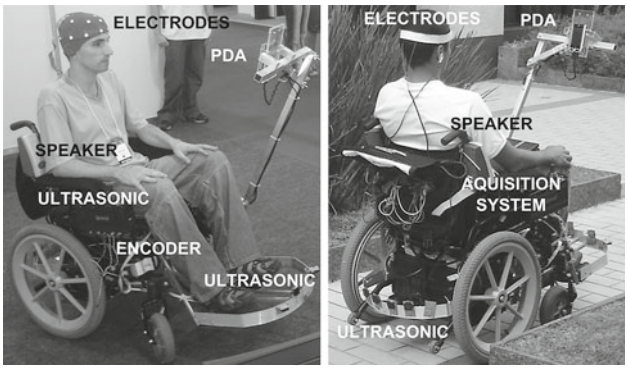

Fig. 1 Robotic wheelchair for people with severe muscular diseases

and/or small, so that the dynamic behavior can be considered approximately as time-invariant. However, this can be a strong supposition for RW applications, where a significant load (their users) can move itself along time. A scheme based on neural networks for adaptive observation of uncertain nonlinear system with time-varying parameters and disturbances is proposed by Vargas and Hemerly (2008).

Safety should be the first concern when designing a RW control system (Fioretti et al. 2000), user comfort being the second one (Ding and Cooper 2005). Therefore, some situations such as abrupt movements and reverse speeds should be avoided. However, trajectory-tracking control strategies, which do not prevent such behaviors by having a strong time restriction, have been considered in recent studies (Cruz et al. 2011a; Martins et al. 2008; Do et al. 2004). Abrupt movements, for instance, are verified when a reference trajectory changes suddenly (yielding high control errors), while reverse speeds are sometimes necessary to reduce such control errors. On the other hand, time restriction is not important in wheelchair applications, which means that trajectory-tracking control is not essential in such cases.

Positioning and path-following controls (de Wit et al. 1997) are strategies with no time restriction. In addition, path-following control (as well as trajectory-tracking) allows to define reference routes in semi-structured known environments, thus minimizing the risk of a collision. So, the path-following control strategy is the most appropriate one for RW applications, being here addressed and highlighted as one contribution of this article.

A classical approach of the path-following problem is given in (de Wit et al. 1997), but it yields to a singular kinematic problem, which is overcome through a small modification proposed in (Soetanto et al. 2003). Both studies propose adaptive control laws based on very simple dynamic models for a wheeled vehicle, but no robustness analysis is performed. A discrete approach is shown in Coelho and Nunes (2005), where a more complete wheelchair dynamic model (with unstructured uncertainties) is considered. The authors apply input-output linearization for specific reference paths, namely, straight lines and circular arcs. Some distinct linear control techniques are used to design robust controllers. However, the great disadvantage of the method is the nonapplicability to complex paths.

Generally, the path-following control laws yet available in the literature neither allow to bound the angular velocity nor take into account the practical limitations of the linear velocity of the mobile vehicles. That is a problem which is solved in this study.

A new RW dynamic model with a mobile load (depicting a person on board) is used in Cruz et al. (2011a), which is an extension of the model obtained for unicycle mobile robots in Martins et al. (2008). An adaptive trajectory-tracking controller based on that model was developed. In Cruz et al. (2011b), a navigation environment of RW structured with metallic paths was proposed, providing greater robustness to the trajectory-tracking system previously proposed. A new approach in this study is done to also insure the robustness of the system for autonomous navigation of RW. The robustness is guaranteed by the path-following controller, so that the path to be followed by RW can be virtually defined based on an environment map previously stored in the system memory, rather than physically constructed such as in Cruz et al. (2011b). Thereby also reduces the need to add a wide range of sensors to the RW (in fact, in this proposal, the vehicle uses only the odometry data to navigate). In addition, it is the first time that such dynamic model is applied to path-following control, allowing a deterministic description of a robust adaptive control system as proposed in the sequel. It should also be stressed that very few studies dealing with robust adaptive control show experimental results, to check the real applicability of the proposed system. This is done here on a RW (Fig. 1), which is thought to be an assistive system capable to navigate autonomously, taking into account the user safety and comfort.

This article is hereinafter organized as follows: the problem formulation is presented in Sect. 2, while Sect. 3 deals with the path-following controller and Sect. 4 shows a proposal for dynamic compensation. Simulation and experimental results are shown and discussed in Sect. 5, and some conclusions are highlighted in Sect. 6.

2 Problem Formulation

Let the motion kinematics be given by

$$\dot{\mathbf{x}} = f\left[\mathbf{x}\left(t\right), \boldsymbol{\phi}\left(t\right)\right] + \boldsymbol{\epsilon}\left(t\right), \ \forall t \geq 0, \tag{1}$$

where $\mathbf{x}$ is a state vector, $\boldsymbol{\phi}$ is a control input vector, f is a known bounded function and $\boldsymbol{\epsilon}$ is an external bounded disturbance vector, with $\mathbf{x}\left(t\right) \in \Re^n$ and $\boldsymbol{\phi}\left(t\right) \in \Re^m$, that is $f : \Re^n \times \Re^m \rightarrow \Re^n$.

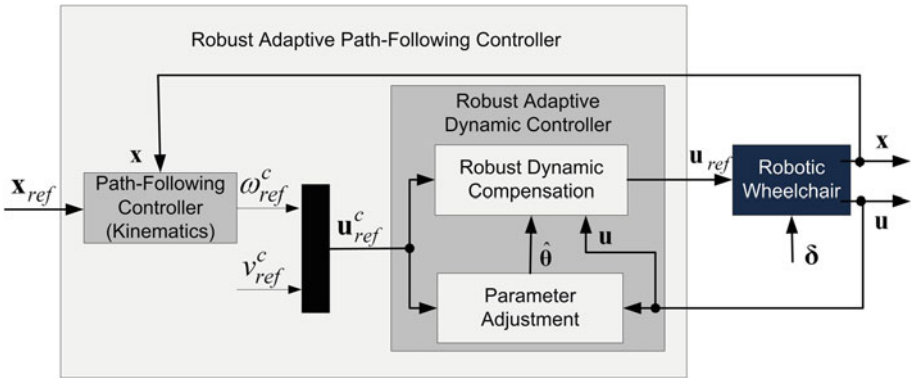

Fig. 2 Block diagram of control structure

Thus, the kinematic control problem here addressed consists in finding a control law $\boldsymbol{\upsilon} = \boldsymbol{\Upsilon}(\mathbf{x})$ that makes $\|\mathbf{x}\| \to x_c$ as $t \to \infty$, with x_c a positive scalar value, that is $0 \leq x_c < \infty$.

Mobile vehicle dynamic effects can be firstly neglected such as in Martins et al. (2008), and Soetanto et al. (2003), allowing to obtain a control law which stabilizes asymptotically a mobile vehicle during reference following, i.e., $x_c = 0$. However, what happens when such effects cannot be neglected? In Martins et al. (2008) it has been prove that when the dynamic effects cannot be neglected and the disturbances $\boldsymbol{\epsilon}$ are bounded, then the system becomes ultimately bounded (i.e., $0 < x_c < \infty$). Such a result allows to consider a cascaded control structure, as shown in Fig. 2. Thus, stability of the kinematic and dynamic controls can be independently verified, simplifying the respective analysis.

One can see in Fig. 2 that the kinematic control receives input signals, $\mathbf{x}_{\text{ref}}$, which describe a desired posture for the mobile vehicle, besides the feedback signals, $\mathbf{x}$, which indicate the current posture of the mobile vehicle. Thus, $\tilde{\mathbf{x}} \equiv \mathbf{x} - \mathbf{x}_{\text{ref}}$ (Fig. 2), or $\tilde{\mathbf{x}} = [\tilde{x}, \tilde{y}, \tilde{\psi}]$, with $\tilde{\psi} \equiv \psi - \psi_{\text{d}}$ (Fig. 3).

It can also be seen that only the angular velocity, $\boldsymbol{\omega}^{\text{c}}_{\text{ref}}$, is generated by the path-following controller. So, the linear velocity, $v^{\text{c}}_{\text{ref}}$, is directly generated (it can be a constant value or conveniently adjusted). Such velocities, i.e., $\mathbf{u}^{\text{c}}_{\text{ref}} = \left[\, v^{\text{c}}_{\text{ref}} \;\; \omega^{\text{c}}_{\text{ref}} \,\right]^T$, are the reference signals applied to the dynamic compensator, while the current velocities, $\mathbf{u}$, of the RW feedbacks such a dynamic controller, forming an inner loop. Figure 2 also shows that the dynamic compensation takes into account parameter uncertainties, by introducing a parameter adjustment, and disturbances $\boldsymbol{\delta}$ (or model uncertainties). Hence, the RW control system is a robust adaptive dynamic one.

3 The Path-Following Controller

The path-following problem formulation here adopted is the same one considered in Soetanto et al. (2003), applicable to any unicycle nonholonomic vehicle. Such a formulation is

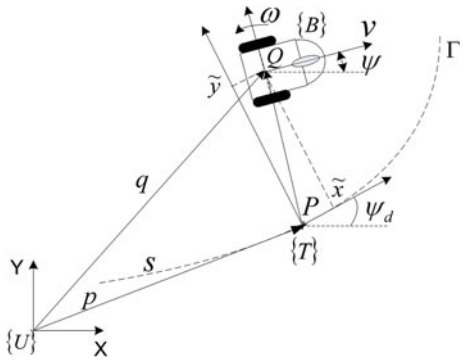

Fig. 3 Path-following problem

illustrated in Fig. 3, where both the vehicle and the reference path, Γ, are represented. There, the frame $\{B\}$, whose origin is the point Q at the middle of the virtual axis connecting the rear wheels of the vehicle, is associated to the mobile vehicle. Linear, v, and angular, ω, velocities are referenced to $\{B\}$. By its turn, P is an arbitrary point of the path Γ being followed, which is the origin of the frame $\{T\}$, s denotes the signed curvilinear abscissa of P along Γ, and $\tilde{x}$ and $\tilde{y}$ are the coordinates in $\{T\}$ of the distance error between Q and P. Finally, ψ is the difference of orientation between $\{B\}$ and the inertial frame $\{U\}$, while ψ_{d} is the difference of orientation between $\{T\}$ and $\{U\}$.

From Fig. 3, one obtains the path-following model Soetanto et al. (2003)

$$\begin{cases} \dot{\tilde{x}} = c(s)\,\tilde{y}\dot{s} - \dot{s} + v\cos\tilde{\psi} \\ \dot{\tilde{y}} = -c(s)\,\tilde{x}\dot{s} + v\sin\tilde{\psi} \\ \dot{\tilde{\psi}} = \omega - c(s)\,\dot{s} \end{cases}, \tag{2}$$

where $\tilde{x}$, $\tilde{y}$ and $\tilde{\psi} \equiv \psi - \psi_{\text{d}}$ are the state variables to be controlled, and $c(s)$ is the path curvature.

The control laws

$$\begin{cases} \dot{s} = v\cos\tilde{\psi} + k_{\tilde{x}}\tilde{x} \\ \dot{\tilde{\psi}} = \dot{\beta} - \gamma\,\tilde{y}v\dfrac{\sin\tilde{\psi} - \sin\beta}{\tilde{\psi} - \beta} - k_{\tilde{\psi}}\left(\tilde{\psi} - \beta\right) \end{cases}, \tag{3}$$

with

$$\beta\left(\tilde{y}, v\right) = -\text{sign}\left(v\right) k_\beta \tanh\left(\tilde{y}\right), \tag{4}$$

are proposed in Soetanto et al. (2003), where $k_{\tilde{x}} \in \Re^+$, $k_{\tilde{\psi}} \in \Re^+$, $\gamma \in \Re^+$ and $k_\beta \in \Re^+$ are design constants. The choice of the function β is instrumental in shaping the transient maneuvers during the path approach phase (Soetanto et al. 2003). The asymptotic stability is proved in such study.

Some modifications in (3) are here proposed, so that

$$\begin{cases} \dot{s} = v\cos\tilde{\psi} + \tilde{X}_{\max}\tanh\left(\frac{k_{\tilde{x}}}{\tilde{X}_{\max}}\tilde{x}\right) \\ \dot{\tilde{\psi}} = \dot{\beta} - \gamma\tilde{y}v\frac{\sin\tilde{\psi}-\sin\beta}{\tilde{\psi}-\beta} - k_{\tilde{\psi}}\left(\tilde{\psi}-\beta\right) \end{cases}, \tag{5}$$

with a variable gain defined as

$$\gamma\left(\tilde{y}\right) \equiv \frac{\Gamma_{\max}}{1+|\tilde{y}|}, \tag{6}$$

are the path-following control laws now considered, where $\tilde{X}_{\max}$ and $\Gamma_{\max}$ are positive saturation constants.

The difference between (3) and (5) is that the first one generates nonbounded control signals, while in our proposal both $\dot{s}$ and $\dot{\tilde{\psi}}$ are bounded for high values of the control errors. One can notice that the function tanh and the variable gain given in (6) make such control signals to be bounded.

To prove the system stability when these new control laws are adopted, it is proposed the Lyapunov function candidate

$$V = \frac{1}{2}\left(\tilde{x}^2 + \tilde{y}^2\right) + \int_0^{\left(\tilde{\psi}-\beta\right)} \frac{1}{\gamma}\alpha\,\mathrm{d}\alpha, \tag{7}$$

where α is an independent variable. Then, taking $\dot{\tilde{x}}$ and $\dot{\tilde{y}}$ from (2) to the first time derivative of (7), and simplifying some terms, one gets

$$\dot{V} = \tilde{x}\left(-\dot{s} + v\cos\tilde{\psi}\right) + \tilde{y}v\sin\tilde{\psi} - \frac{1}{\gamma}\left(\tilde{\psi}-\beta\right)\left(\dot{\tilde{\psi}}-\dot{\beta}\right). \tag{8}$$

Reverse speeds are not recommended in RW applications, because they are very uncomfortable for the user. Moreover, such kind of movements makes it necessary to add expensive back sensing subsystem to guarantee the system safety. Hence, it is desirable that only positive linear velocities be sent as references to RWs, allowing to rewrite (4) as

$$\beta\left(\tilde{y}\right) = -k_\beta \tanh\left(\tilde{y}\right), \tag{9}$$

so that $\dot{\beta}$ exists for all time.

Now, by replacing (5) into (8), one obtains

$$\dot{V} = -\tilde{x}\tilde{X}_{\max}\tanh\left(\frac{k_{\tilde{x}}}{\tilde{X}_{\max}}\tilde{x}\right) + \tilde{y}v\sin\beta - \frac{1}{\gamma}\left(\tilde{\psi}-\beta\right)^2. \tag{10}$$

From (9), one can verify that $\tilde{y}v\sin\beta < 0,\ \forall\ \tilde{y} \neq 0$, so that (10) is a negative function $\forall\ \tilde{x} \neq 0, \forall\ \tilde{y} \neq 0$ and $\forall\ \tilde{\psi} \neq 0$. So, the asymptotic stability is proven.

The input commands are the linear and angular reference velocities given by

$$\begin{cases} v_{\text{ref}}^{\text{c}} = v_{\text{ref}}^{\text{c}}\left(\cdot\right) \\ \omega_{\text{ref}}^{\text{c}} = \dot{\tilde{\psi}} + \text{c}\dot{s} \end{cases}, \tag{11}$$

where $v_{\text{ref}}^{\text{c}}\left(\cdot\right)$ is a positive function and $\omega_{\text{ref}}^{\text{c}}$ is obtained by replacing the control laws given in (5) into the last equation of (2).

4 Dynamic Control

4.1 Robotic Wheelchair Dynamic Model and Its Properties

RWs are mobile vehicles with a special dynamic characteristic due to the presence of a person on board, which represents a heavy and mobile load. RWs have nominal mass equal approximately to 70 kg and their maximum payload is 130 kg. That is an extra mass nearly twice the vehicle nominal mass which can change its position on the vehicle. Figure 4 depicts a loaded RW, for which B is the point in the middle of the virtual axis linking the rear wheels and G is the center of mass which can be displaced from B by the distances b_1 and b_2, not necessarily constant.

From such considerations, it was proposed in Cruz et al. (2011a) a RW dynamic model, which also takes into account external forces and torques, and the presence of low level controllers. The model is given by

$$\mathbf{M}\dot{\mathbf{u}}\left(t\right) + \mathbf{C}\mathbf{u}\left(t\right) + \boldsymbol{\delta}\left(t\right) = \mathbf{u}_{\text{ref}}\left(t\right), \tag{12}$$

where $\mathbf{u} = \left[v\ \omega\right]^T$ and $\mathbf{u}_{\text{ref}} = \left[v_{\text{ref}}\ \omega_{\text{ref}}\right]^T$ are the response and reference velocity vectors, respectively, $\boldsymbol{\delta} = \left[-\delta_v\ -\delta_\omega\right]^T$ is the disturbance vector,

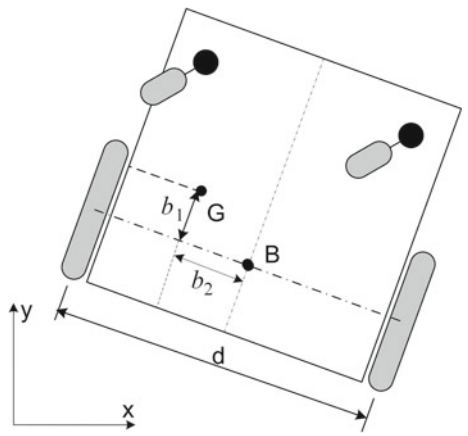

Fig. 4 Displacement of center of mass on a RW

$$\mathbf{M} = \begin{bmatrix} \theta_1 & -\theta_7 \\ -\theta_8 & \theta_2 \end{bmatrix} \text{ and } \mathbf{C} = \begin{bmatrix} \theta_4 & -\theta_3\omega \\ \theta_5\omega & \theta_6 \end{bmatrix} \tag{13}$$

are dynamic parameter matrices, for which

$$\begin{cases} \theta_1 = \frac{k_{DT}}{k_{PT}} + \frac{R_a r}{2k_{PT}k_a}\left(\frac{2I_a}{r^2} + m\right) \\ \theta_2 = \frac{k_{DR}}{k_{PR}} + \frac{R_a r}{k_{PR}k_a d}\left(\frac{I_a d^2}{2r^2} + I_z + m\left(b_1^2 + b_2^2\right)\right) \\ \theta_3 = \frac{R_a r m b_1}{2k_{PT}k_a} \\ \theta_4 = 1 + \frac{k_a}{k_{PT}r} + \frac{B_a R_a}{k_{PT}k_a r} \\ \theta_5 = \frac{R_a r b_1 m}{d k_{PR} k_a} \\ \theta_6 = 1 + \frac{d k_b}{2r k_{PR}} + \frac{R_a B_e d}{2r k_{PR} k_a} \\ \theta_7 = \frac{b_2 m R_a r}{2k_{PT}k_a} \\ \theta_8 = \frac{b_2 m R_a r}{k_{PR} d k_a} \end{cases}, \tag{14}$$

m being the mass of both RW and passenger, k_{PT}, k_{DT}, k_{PR} and k_{DR} being low level control gains, responsible for controlling the angular velocity of the RW driven wheels dos Santos Filgueira (2011). I_e and B_e are the moment of inertia and the viscous friction coefficient of the combined motor rotor, gearbox and wheel, I_z is the moment of inertia at the vertical axis located on G, k_b is equal to the voltage constant multiplied by the gear ratio, R_a is the motor electric resistance, k_a is the torque constant also multiplied by the gear ratio, r is the radius of the traction wheels, and d is the distance between the traction wheels.

Remark 1 Although the greater part of the physical parameters, $\boldsymbol{\theta}$, is constant, it should be considered that some parameters, such as mass m and the displacement of the center of mass G, given by b_1 and b_2, can suffer changes because of being associated to the presence of a person on board. Consequently, almost all parameters are subject to changes, according to (14).

By rearranging the terms, one can express (12) as

$$\mathrm{T}\boldsymbol{\theta}(t) + \boldsymbol{\delta}(t) = \mathbf{u}_{\text{ref}}, \tag{15}$$

where $\mathrm{T} = \begin{bmatrix} \dot{v} & 0 & -\omega^2 & v & 0 & 0 & -\dot{\omega} & 0 \\ 0 & \dot{\omega} & 0 & 0 & v\omega & \omega & 0 & -\dot{v} \end{bmatrix}$ and $\boldsymbol{\theta}(t) = [\theta_1 \quad \theta_2 \quad \ldots \quad \theta_8]^T$. Moreover, (12) can be rewritten as

$$\mathbf{M}(t)\dot{\mathbf{u}} + \boldsymbol{\eta} + \boldsymbol{\delta} = \mathbf{u}_{\text{ref}}, \tag{16}$$

with

$$\boldsymbol{\eta} = \begin{bmatrix} 0 & 0 & -\omega^2 & v & 0 & 0 & 0 & 0 \\ 0 & 0 & 0 & 0 & v\omega & \omega & 0 & 0 \end{bmatrix}\boldsymbol{\theta}(t). \tag{17}$$

Remark 2 In the sequel we will use the notation $\boldsymbol{\theta}(t) = \boldsymbol{\theta}$ and $\boldsymbol{M}(t) = \boldsymbol{M}$.

The parameters included in the vector $\boldsymbol{\theta}$ are functions of some physical parameters of the RW, which can be estimated by neglecting the disturbance vector, $\boldsymbol{\delta}$, in (15), that is

$$\mathrm{T}\hat{\boldsymbol{\theta}} = \mathbf{u}_{\text{ref}}, \tag{18}$$

where $\hat{\boldsymbol{\theta}}$ is the estimate parameters vector, T is the regression matrix and $\mathbf{u}_{\text{ref}}$ is the output vector (Cruz and Carelli 2006; Aström and Wittenmark 2008).

The following model properties will be used in the sequel.

1. $\theta_1 > 0,\ \theta_2 > 0,\ \theta_4 > 0$ and $\theta_6 > 0$;
2. sign (θ_7) = sign (θ_8);
3. sign $(\dot{\theta}_7)$ = sign $(\dot{\theta}_8)$;
4. $\theta_1\theta_2 > \theta_7\theta_8$;
5. $\boldsymbol{M}$ is a diagonalizable positive definite matrix;
6. $\dot{\boldsymbol{M}}$ is a diagonalizable matrix;
7. Every column vector that compose $\mathbf{T}$ has only one variable element and the remaining elements are zero.

Proof Except for b_1 and b_2 which can be positive, negative, or null, all physical parameters are always positive. Thus, Properties 1–3 are straightforwardly checked using (14).

Continuing the analysis of the above properties, one can check that

$$\det(\mathbf{M}) = \theta_1\theta_2 - \theta_7\theta_8 = \left(\frac{k_{DT}}{k_{PT}} + \frac{R_a I_e}{r k_{PT} k_a}\right) \times \left(\frac{k_{DR}}{k_{PR}} + \frac{R_a r}{d k_{PR} k_a}\left(\frac{I_e d^2}{2rr} + I_z + m b_1^2\right)\right) > 0 \tag{19}$$

(because of all physical parameters involved being positive), thus verifying Property 4. To check Property 5, one should firstly calculate the eigenvalues of $\mathbf{M}$, which are

$$\begin{cases} \lambda_1 = \frac{1}{2}\left(\theta_1 + \theta_2 + \sqrt{(\theta_1 - \theta_2)^2 + 4\theta_7\theta_8}\right) \\ \lambda_2 = \frac{1}{2}\left(\theta_1 + \theta_2 - \sqrt{(\theta_1 - \theta_2)^2 + 4\theta_7\theta_8}\right) \end{cases}. \tag{20}$$

Then, knowing that Properties 1, 2 and 4 are valid, one can conclude that $\lambda_1 \in \Re^+$ and $\lambda_2 \in \Re^+$ (because the term inside the square root is positive), and $\lambda_1 \neq \lambda_2$. In addition, $\mathbf{M}$ is symmetric ($\theta_7 = \theta_8$), since $\frac{k_{PT}}{k_{PR}} = \frac{d}{2}$. Thus, the low level control gains are suitably adjusted to make the matrix $\mathbf{M}$ symmetric, leading to the conclusion that $\mathbf{M}$ is a positive definite matrix [see Strang (1988)], i.e., the Property 5 is also verified.

From (13), it implies that

$$\dot{\mathbf{M}} = \begin{bmatrix} \dot{\theta}_1 & -\dot{\theta}_7 \\ -\dot{\theta}_8 & \dot{\theta}_2 \end{bmatrix},$$

eigenvalues of which Sare given by

$$\begin{cases} \lambda_3 = \frac{1}{2}\left(\dot{\theta}_1 + \dot{\theta}_2 + \sqrt{\left(\dot{\theta}_1 - \dot{\theta}_2\right)^2 + 4\dot{\theta}_7\dot{\theta}_8}\right) \\ \lambda_4 = \frac{1}{2}\left(\dot{\theta}_1 + \dot{\theta}_2 - \sqrt{\left(\dot{\theta}_1 - \dot{\theta}_2\right)^2 + 4\dot{\theta}_7\dot{\theta}_8}\right) \end{cases}. \tag{21}$$

Considering the Property 3, one can verify that $\lambda_3 \in \Re$ and $\lambda_4 \in \Re$. Moreover, such eigenvalues are visibly distinct. Hence, $\dot{\mathbf{M}}$ is a diagonalizable matrix (Strang 1988). Notice, however, that property 6 is valid only when $\dot{\mathbf{M}} \neq 0$.

Finally, the definition of the matrix $\mathbf{T}$ in (15) reveals the property 7.

4.2 Robust Adaptive Dynamic Control

From (16), it is used the dynamic control law

$$\mathbf{u}_{\text{ref}} = \mathbf{M}\boldsymbol{\sigma} + \boldsymbol{\eta} + \mathbf{K}_{\text{r}}\text{sign}\left(\tilde{\mathbf{u}}\right), \tag{22}$$

which is based on the dynamic control law for robot manipulators proposed by Slotine and Li (1988). In Eq. (22), $\mathbf{K}_{\text{r}} = \text{diag}\left(k_{\text{r}v}, k_{\text{r}\omega}\right) > 0$ and

$$\boldsymbol{\sigma} = \dot{\mathbf{u}}_{\text{ref}}^{\text{c}} + \mathbf{K}\tilde{\mathbf{u}}, \tag{23}$$

being $\mathbf{K} = \text{diag}\left(k_v, k_\omega\right) > 0$ and $\tilde{\mathbf{u}} = \mathbf{u}_{\text{ref}}^{\text{c}} - \mathbf{u}$, where the superscript c indicates that the signals are coming from a kinematic controller, as shown in Fig. 2. However, $\dot{\mathbf{u}}_{\text{ref}}^{\text{c}}$ should be derived from the output velocities of the path-following controller.

Based on (15), Eq. (22) can also be written as

$$\mathbf{u}_{\text{ref}} = \mathbf{T}\left(\boldsymbol{\sigma}, \mathbf{u}\right)\boldsymbol{\theta} + \mathbf{K}_{\text{r}}\text{sign}\left(\tilde{\mathbf{u}}\right), \tag{24}$$

where

$$\mathbf{T}\left(\boldsymbol{\sigma}, \mathbf{u}\right) = \begin{bmatrix} \sigma_v & 0 & -\omega^2 v & 0 & 0 & -\sigma_\omega & 0 \\ 0 & \sigma_\omega & 0 & 0\, v\omega\, \omega & 0 & & -\sigma_v \end{bmatrix}.$$

The last term in the right side of (22) and (24) is a robustness term, to reduce the model uncertainty [given by $\boldsymbol{\delta}$ in (16)] due to disturbances and nonmodeled dynamic effects.

Supposing that there also exists some uncertainty in the identifiable parameters, the dynamic control law

$$\mathbf{u}_{\text{ref}} = \mathbf{T}\hat{\boldsymbol{\theta}} + \mathbf{K}_{\text{r}}\text{sign}\left(\tilde{\mathbf{u}}\right) \tag{25}$$

should be considered, instead of (22) or (24), where

$$\hat{\boldsymbol{\theta}} \equiv \boldsymbol{\theta} + \tilde{\boldsymbol{\theta}} \tag{26}$$

is the vector of estimated parameters and $\tilde{\boldsymbol{\theta}} \in \Re^8$ is the vector of parameter errors.

Replacing (26) in (25) one gets

$$\mathbf{u}_{\text{ref}} = \mathbf{T}\boldsymbol{\theta} + \mathbf{T}\tilde{\boldsymbol{\theta}} + \mathbf{K}_{\text{r}}\text{sign}\left(\tilde{\mathbf{u}}\right) \tag{27}$$

or

$$\mathbf{u}_{\text{ref}} = \mathbf{M}\boldsymbol{\sigma} + \boldsymbol{\eta} + \mathbf{T}\tilde{\boldsymbol{\theta}} + \mathbf{K}_{\text{r}}\text{sign}\left(\tilde{\mathbf{u}}\right). \tag{28}$$

From (16) and (28), it follows that

$$\mathbf{M}\dot{\mathbf{u}} + \boldsymbol{\eta} + \boldsymbol{\delta} = \mathbf{M}\boldsymbol{\sigma} + \boldsymbol{\eta} + \mathbf{T}\tilde{\boldsymbol{\theta}} + \mathbf{K}_{\text{r}}\text{sign}\left(\tilde{\mathbf{u}}\right), \tag{29}$$

which is equivalent to

$$\mathbf{M}\left(\boldsymbol{\sigma} - \dot{\mathbf{u}}\right) = \boldsymbol{\delta} - \mathbf{T}\tilde{\boldsymbol{\theta}} - \mathbf{K}_{\text{r}}\text{sign}\left(\tilde{\mathbf{u}}\right). \tag{30}$$

From (23), one gets $\boldsymbol{\sigma} - \dot{\mathbf{u}} = \dot{\tilde{\mathbf{u}}} + \mathbf{K}\tilde{\mathbf{u}}$, which is used in (30), resulting in the tracking error

$$\dot{\tilde{\mathbf{u}}} = \mathbf{M}^{-1}\left(\boldsymbol{\delta} - \mathbf{T}\tilde{\boldsymbol{\theta}} - \mathbf{K}_{\text{r}}\text{sign}\left(\tilde{\mathbf{u}}\right)\right) - \mathbf{K}\tilde{\mathbf{u}}. \tag{31}$$

Since $\mathbf{M} > 0$ (Property 5), then $\exists\,\mathbf{M}^{-1}$. That is, the error function given in (31) is a nonsingular one.

In the sequel, it is defined

$$\mathbf{P} \equiv \begin{bmatrix} 2k_{\text{PT}} & 0 \\ 0 & dk_{\text{PR}} \end{bmatrix} > 0 \tag{32}$$

(formed by constant parameters of the RW), which makes the product $\mathbf{PM}$ a positive definite symmetric matrix. Subsequently, Property 7 is considered to introduce the following proposition:

Proposition 1 $\mathbf{T}\bar{\mathbf{P}} = \mathbf{P}\mathbf{T}$, *with* $\bar{\mathbf{P}} = \text{diag}\left(\bar{p}_1, \ldots, \bar{p}_8\right)$.

As a result of (32) and Proposition 1, one gets $\bar{\mathbf{P}} > 0$. Thus,

$$V = \frac{1}{2}\tilde{\mathbf{u}}^T\mathbf{P}\mathbf{M}\tilde{\mathbf{u}} + \frac{1}{2}\tilde{\boldsymbol{\theta}}^T\bar{\mathbf{P}}\boldsymbol{\Xi}\tilde{\boldsymbol{\theta}} \tag{33}$$

is a Lyapunov candidate function, where $\boldsymbol{\Xi} \in \Re^{8\times 8}$ is a positive definite diagonal matrix.

Assumption 1 The dynamic parameters are time-varying, i.e., $\boldsymbol{\theta} = \boldsymbol{\theta}\left(t\right)$ and $\mathbf{M} = \mathbf{M}\left(t\right)$.

Then, the first time derivative of (33) is

$$\dot{V} = \tilde{\mathbf{u}}^T\mathbf{P}\mathbf{M}\dot{\tilde{\mathbf{u}}} + \frac{1}{2}\tilde{\mathbf{u}}^T\mathbf{P}\dot{\mathbf{M}}\tilde{\mathbf{u}} + \tilde{\boldsymbol{\theta}}^T\bar{\mathbf{P}}\boldsymbol{\Xi}\dot{\tilde{\boldsymbol{\theta}}}. \tag{34}$$

Considering (31), Eq. (34) becomes

$$\begin{aligned}\dot{V} = &-\tilde{\mathbf{u}}^T\mathbf{P}\mathbf{M}\mathbf{K}\tilde{\mathbf{u}} - \tilde{\mathbf{u}}^T\mathbf{P}\mathbf{T}\tilde{\boldsymbol{\theta}} - \tilde{\mathbf{u}}^T\mathbf{P}\mathbf{K}_{\text{r}}\text{sign}\left(\tilde{\mathbf{u}}\right) \\ &+\tilde{\mathbf{u}}^T\mathbf{P}\boldsymbol{\delta} + \frac{1}{2}\tilde{\mathbf{u}}^T\mathbf{P}\dot{\mathbf{M}}\tilde{\mathbf{u}} + \tilde{\boldsymbol{\theta}}^T\bar{\mathbf{P}}\boldsymbol{\Xi}\dot{\tilde{\boldsymbol{\theta}}},\end{aligned} \tag{35}$$

where $\mathbf{PMK} \in \Re^{2x2}$ is not necessarily symmetric. However, such a matrix keeps the properties of the matrix $\mathbf{M}$, i.e., it is a diagonalizable positive definite one. Furthermore, $\mathbf{P}\dot{\mathbf{M}}$ is a diagonalizable matrix (see proofs of Properties 5 and 6).

In the sequel, it is proposed the parameter updating law

$$\dot{\hat{\boldsymbol{\theta}}} = \boldsymbol{\Xi}^{-1}\left(\mathbf{T}^T\tilde{\mathbf{u}} - \boldsymbol{\Gamma}\hat{\boldsymbol{\theta}}\right), \tag{36}$$

where $\boldsymbol{\Gamma} \in \Re^{8\times 8}$ is a positive definite diagonal matrix.

From (36), one can first observe that the parameter adjustment depends on the tracking errors, which are clearly affected by parameter errors $\tilde{\boldsymbol{\theta}}$, as it can be seen in (31). Moreover, the last term of (36) introduces a negative feedback on the estimated parameters, to avoid parameter drift due to measurement errors, noise, and/or disturbances (Aström and Wittenmark 2008). Such a technique is known in the literature as σ-modification or leakage-term (Sastry and Bodson 1989).

Now, from (26) and considering Assumption 1, it follows that

$$\dot{\tilde{\boldsymbol{\theta}}} = \dot{\hat{\boldsymbol{\theta}}} - \dot{\boldsymbol{\theta}}. \tag{37}$$

By substituting (36) into (37), and considering (26), it results that

$$\dot{\tilde{\boldsymbol{\theta}}} = \boldsymbol{\Xi}^{-1}\left(\mathbf{T}^T\tilde{\mathbf{u}} - \boldsymbol{\Gamma}\tilde{\boldsymbol{\theta}} - \boldsymbol{\Gamma}\boldsymbol{\theta}\right) - \dot{\boldsymbol{\theta}}, \tag{38}$$

which, introduced in (35), leads to

$$\begin{aligned}\dot{V} = &-\tilde{\mathbf{u}}^T\mathbf{H}\tilde{\mathbf{u}} - \tilde{\boldsymbol{\theta}}^T\bar{\boldsymbol{\Gamma}}\tilde{\boldsymbol{\theta}} - \tilde{\mathbf{u}}^T\bar{\mathbf{K}}_{\mathrm{r}}\mathrm{sign}\left(\tilde{\mathbf{u}}\right) + \tilde{\mathbf{u}}^T\bar{\boldsymbol{\delta}}\\ &-\tilde{\boldsymbol{\theta}}^T\bar{\boldsymbol{\Gamma}}\boldsymbol{\theta} - \tilde{\boldsymbol{\theta}}^T\bar{\boldsymbol{\Xi}}\dot{\boldsymbol{\theta}} + \frac{1}{2}\tilde{\mathbf{u}}^T\boldsymbol{\Pi}\tilde{\mathbf{u}},\end{aligned} \tag{39}$$

where $\mathbf{H} = \mathbf{PMK}$, $\boldsymbol{\Pi} = \mathbf{P}\dot{\mathbf{M}}$, $\bar{\boldsymbol{\Gamma}} = \bar{\mathbf{P}}\boldsymbol{\Gamma}$, $\bar{\mathbf{K}}_{\mathrm{r}} = \mathbf{PK}_{\mathrm{r}}$, $\bar{\boldsymbol{\delta}} = \mathbf{P}\boldsymbol{\delta}$ and $\bar{\boldsymbol{\Xi}} = \bar{\mathbf{P}}\boldsymbol{\Xi}$.

Now, let the constants $\mu_{\mathrm{Hmin}} = \sqrt{\lambda_{\min}\left(\mathbf{H}^T\mathbf{H}\right)}$, $\mu_{\mathrm{Krmin}} = \sqrt{\lambda_{\min}\left(\bar{\mathbf{K}}_{\mathrm{r}}^T\bar{\mathbf{K}}_{\mathrm{r}}\right)}$ and $\mu_{\Gamma\mathrm{min}} = \sqrt{\lambda_{\min}\left(\bar{\boldsymbol{\Gamma}}^T\bar{\boldsymbol{\Gamma}}\right)}$ be the smallest singular values of the matrices $\mathbf{H}$, $\bar{\mathbf{K}}_r$ and $\bar{\boldsymbol{\Gamma}}$, and $\mu_{\Gamma\mathrm{max}} = \sqrt{\lambda_{\max}\left(\bar{\boldsymbol{\Gamma}}^T\bar{\boldsymbol{\Gamma}}\right)}$, $\mu_{\Xi\mathrm{max}} = \sqrt{\lambda_{\max}\left(\bar{\boldsymbol{\Xi}}^T\bar{\boldsymbol{\Xi}}\right)}$ and $\mu_{\Pi\mathrm{max}} = \sqrt{\lambda_{\max}\left(\boldsymbol{\Pi}^T\boldsymbol{\Pi}\right)}$ be the largest singular values of the matrices $\bar{\boldsymbol{\Gamma}}$, $\bar{\boldsymbol{\Xi}}$ and $\boldsymbol{\Pi}$, being $\lambda_{\min}(\cdot)$ and $\lambda_{\max}(\cdot)$ the smallest and the largest eigenvalues of a matrix. Thus, from (39) one gets

$$\begin{aligned}\dot{V} \leq &-\left(\mu_{\mathrm{Hmin}} - \frac{1}{2}\mu_{\Pi\mathrm{max}}\right)\|\tilde{\mathbf{u}}\|^2 - \mu_{\Gamma\mathrm{min}}\left\|\tilde{\boldsymbol{\theta}}\right\|^2 - (\mu_{\mathrm{Krmin}}\\ &-\left\|\bar{\boldsymbol{\delta}}\right\|)\|\tilde{\mathbf{u}}\| + \mu_{\Gamma\mathrm{max}}\left\|\tilde{\boldsymbol{\theta}}\right\|\|\boldsymbol{\theta}\| + \mu_{\Xi\mathrm{max}}\left\|\tilde{\boldsymbol{\theta}}\right\|\|\dot{\boldsymbol{\theta}}\|.\end{aligned} \tag{40}$$

Considering the squared difference

$$\left(\frac{1}{\xi}\left\|\tilde{\boldsymbol{\theta}}\right\| - \xi\|\boldsymbol{\theta}\|\right)^2 = \frac{1}{\xi^2}\left\|\tilde{\boldsymbol{\theta}}\right\|^2 - 2\left\|\tilde{\boldsymbol{\theta}}\right\|\|\boldsymbol{\theta}\| + \xi^2\|\boldsymbol{\theta}\|^2, \tag{41}$$

with $\xi \in \Re^+$, one can write

$$\left\|\tilde{\boldsymbol{\theta}}\right\|\|\boldsymbol{\theta}\| = \frac{1}{2\xi^2}\left\|\tilde{\boldsymbol{\theta}}\right\|^2 + \frac{\xi^2}{2}\|\boldsymbol{\theta}\|^2 - \frac{1}{2}\left(\frac{1}{\xi}\left\|\tilde{\boldsymbol{\theta}}\right\| - \xi\|\boldsymbol{\theta}\|\right)^2. \tag{42}$$

By neglecting the negative term in (42), the inequality

$$\left\|\tilde{\boldsymbol{\theta}}\right\|\|\boldsymbol{\theta}\| \leq \frac{1}{2\xi^2}\left\|\tilde{\boldsymbol{\theta}}\right\|^2 + \frac{\xi^2}{2}\|\boldsymbol{\theta}\|^2, \tag{43}$$

is obtained. By applying a similar reasoning, one also gets

$$\left\|\tilde{\boldsymbol{\theta}}\right\|\|\dot{\boldsymbol{\theta}}\| \leq \frac{1}{2\chi^2}\left\|\tilde{\boldsymbol{\theta}}\right\|^2 + \frac{\chi^2}{2}\|\dot{\boldsymbol{\theta}}\|^2, \tag{44}$$

with $\chi \in \Re^+$. Then, replacing (43) and (44) in (40), one gets

$$\begin{aligned}\dot{V} \leq &-\left(\mu_{\mathrm{Hmin}} - \frac{1}{2}\mu_{\Pi\mathrm{max}}\right)\|\tilde{\mathbf{u}}\|^2\\ &-\left(\mu_{\Gamma\mathrm{min}} - \frac{\mu_{\Gamma\mathrm{max}}}{2\xi^2} - \frac{\mu_{\Xi\mathrm{max}}}{2\chi^2}\right)\left\|\tilde{\boldsymbol{\theta}}\right\|^2\\ &-\left(\mu_{\mathrm{Krmin}} - \left\|\bar{\boldsymbol{\delta}}\right\|\right)\|\tilde{\mathbf{u}}\|\\ &+\left(\mu_{\Gamma\mathrm{max}}\frac{\xi^2}{2}\|\boldsymbol{\theta}\|^2 + \mu_{\Xi\mathrm{max}}\frac{\chi^2}{2}\left\|\dot{\boldsymbol{\theta}}\right\|^2\right).\end{aligned} \tag{45}$$

Defining

$$\alpha_1 \equiv \mu_{\mathrm{Hmin}} - \frac{1}{2}\mu_{\Pi\mathrm{max}}, \tag{46}$$

$$\alpha_2 \equiv \mu_{\Gamma\mathrm{min}} - \frac{\mu_{\Gamma\mathrm{max}}}{2\xi^2} - \frac{\mu_{\Xi\mathrm{max}}}{2\chi^2}, \tag{47}$$

$$\alpha_3 \equiv \mu_{\mathrm{Krmin}} - \mathrm{sign}\left(\tilde{\mathbf{u}}\right)\|\bar{\boldsymbol{\delta}}\| \tag{48}$$

and

$$\rho \equiv \mu_{\Gamma\mathrm{max}}\frac{\xi^2}{2}\|\boldsymbol{\theta}\|^2 + \mu_{\Xi\mathrm{max}}\frac{\chi^2}{2}\left\|\dot{\boldsymbol{\theta}}\right\|^2, \tag{49}$$

then

$$\dot{V} \leq -\alpha_1\|\tilde{\mathbf{u}}\|^2 - \alpha_2\left\|\tilde{\boldsymbol{\theta}}\right\|^2 - \alpha_3\|\tilde{\mathbf{u}}\| + \rho. \tag{50}$$

It can be observed in (46) that the constant α_1 is positive, as $\mu_{\mathrm{Hmin}} > \frac{1}{2}\mu_{\Pi\mathrm{max}}$, thus establishing a minimum value for the proporcional gains of the control signals, given in (23), which act on the tracking errors. One observes in (47) that the constant α_2 is positive as $\mu_{\Gamma\mathrm{min}} - \frac{\mu_{\Gamma\mathrm{max}}}{2\xi^2} > \frac{\mu_{\Xi\mathrm{max}}}{2\chi^2}$ (that is possible for ξ and χ conveniently selected), establishing minimum and maximum values for the parameter updating law given in (36). Finally, it can be seen in (48) that the constant α_3 is positive as $\mu_{\mathrm{Krmin}} > \|\bar{\boldsymbol{\delta}}\|$. So, a minimum value for the gains associated to the robustness term embedded in the dynamic compensation law, given in (25), is also established. Hence, it is necessary to assume that the amplified disturbances, $\bar{\boldsymbol{\delta}}$, are physically bounded, i.e., $\|\bar{\boldsymbol{\delta}}\| \leq \Delta$, with $0 \leq \Delta < \infty$.

Then, it is possible to guarantee that the three first terms of (50) are strictly negative. On the other hand, the last term of (50) is strictly positive, according to (49). But ρ depends on the dynamic parameters of the system, $\boldsymbol{\theta}(t)$, and their first time derivative, $\dot{\boldsymbol{\theta}}(t)$, which are physically bounded, making ρ a bounded variable. That leads us to conclude, through (50), that $\tilde{\mathbf{u}}$ and $\tilde{\boldsymbol{\theta}}$ are ultimately bounded errors since gains and constants of the robust adaptive dynamic controller are required to be carefully adjusted.

One can observe in (49) that ρ can be selected as small as desired by choosing gains for $\boldsymbol{\Gamma}$ and $\boldsymbol{\Xi}$ sufficiently small. However, very small gains can cause robustness problems, known as parameter drift (Aström and Wittenmark 2008).

The reader should also notice that the proposed controller does not guarantee that $\tilde{\boldsymbol{\theta}}(t) \to 0$ as $t \to \infty$. It only guarantees that the parameter error is bounded. Actually, it is not required that $\tilde{\boldsymbol{\theta}}(t) \to 0$ to make $\tilde{\mathbf{u}}$ to converge to a bounded value.

5 Results

The path-following controller proposed in Soetanto et al. (2003), whose control laws are shown in (3), is first considered. The controller gains were conveniently adjusted when

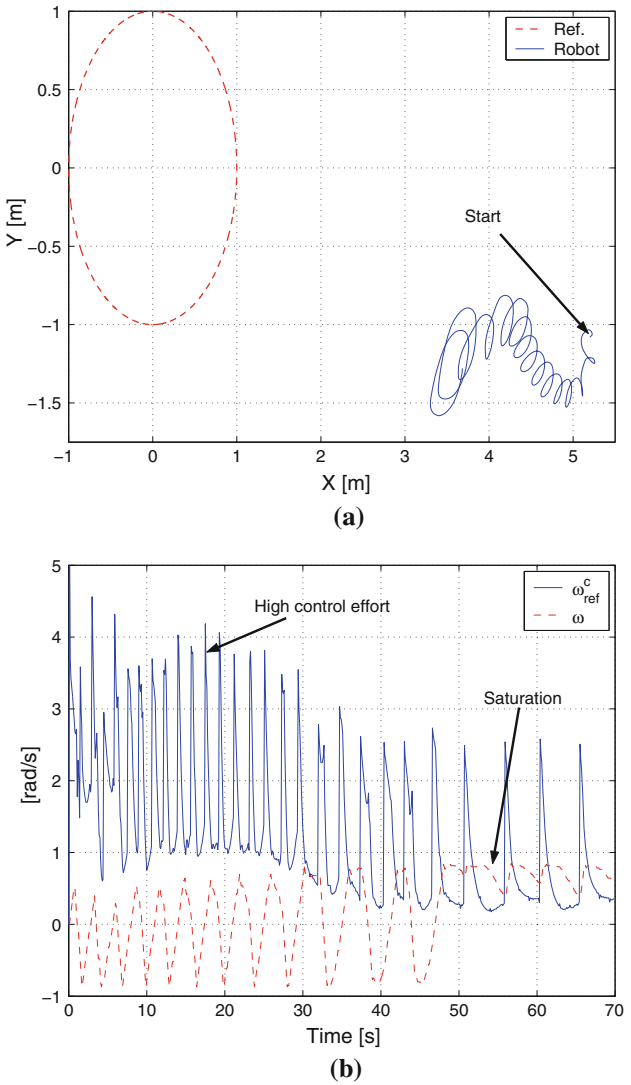

Fig. 5 Simulated case: unstable vehicle due to saturation effects

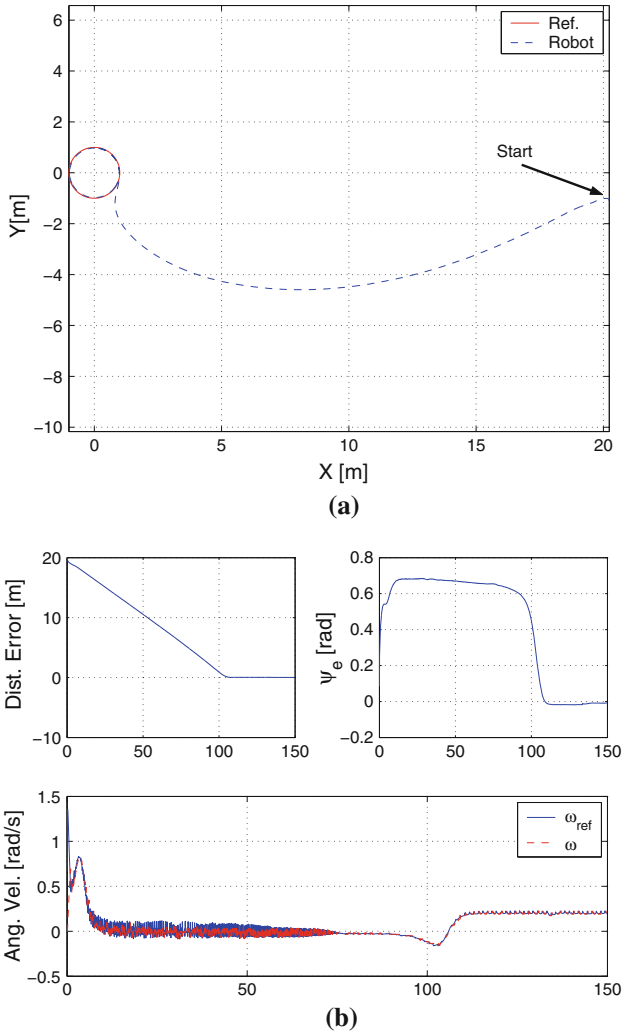

Fig. 6 Simulated case: without saturation effects

distance errors are small (lower than $2m$), so that $k_{\tilde{x}} = 1$, $k_{\tilde{\psi}} = 5$, $\gamma = 3$ and $k_\beta = \pi/4$. Then, simulations with the vehicle starting far from the reference path were carried out. Figure 5a shows a bad result when the mobile vehicle starts at a position approximately $5m$ distant from the reference path. In this case, a high control effort followed by saturation effect (Fig. 5b) were sufficiently strong to make the vehicle unstable.

The same procedure was performed considering the modified controller presented in (5), i.e., simulations with the mobile vehicle starting significantly distant from the reference path. Figure 6 shows a good behavior when the vehicle starts at a position approximately 20 m distant from the reference path. The gain values were kept, allowing a performance comparison between both controllers. The saturation constants introduced into the last controller are $X_{\max} = 1$ and $\Gamma_{\max} = 3$.

Experiments performed on a RW allowed to complete the validation of the proposed controller. The same values of gains and saturation constants were adopted for the simulations and experiments hereinafter described. Figure 7 shows that the mobile vehicle, initially positioned approximately 4 m away of the reference path, effectively reaches such path and follows it.

Simulations using the dynamic model given in (12) were carried out to emphasize the importance of a robust adaptive dynamic control when the system has structured uncertainties, unstructured uncertainties and time-varying parameters. Figure 8 shows a RW carrying a heavy person (125 kg), for which the values identified for the model parameters are $\theta_1 = 0.3241$, $\theta_2 = 0.0120$, $\theta_3 = 0.0092$, $\theta_4 = 0.9969$, $\theta_5 = 0.0634$, $\theta_6 = 0.9898$, $\theta_7 = -0.0562$ and $\theta_8 = -0.0002$. Such parameter values were loaded into a RW simulator. On the other hand, parameters corresponding to the wheelchair without any user are considered as initial estimates for the

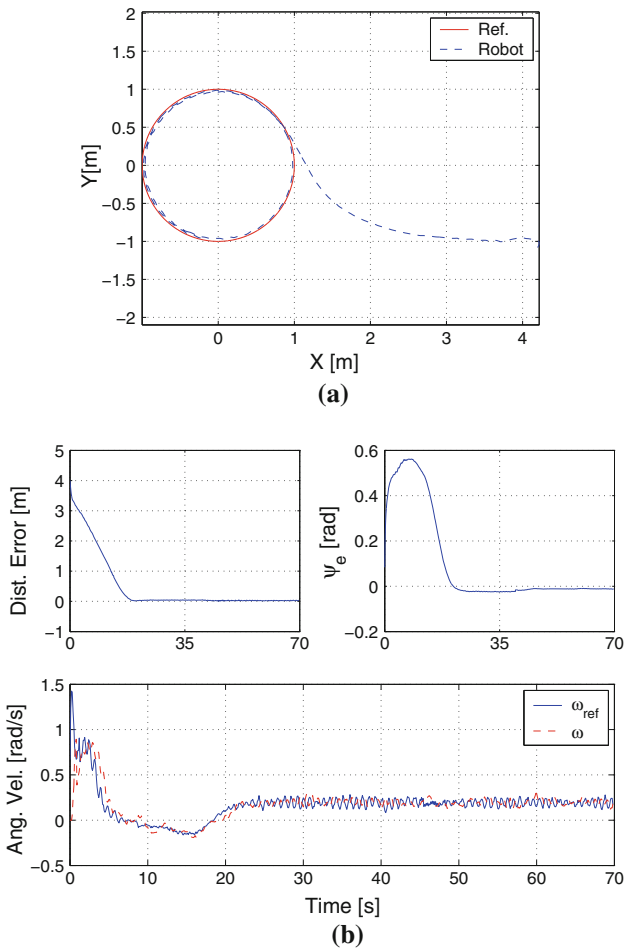

Fig. 7 Experiment: the robot's initial position is far from the reference path

Fig. 8 A robotic wheelchair carrying a heavy person

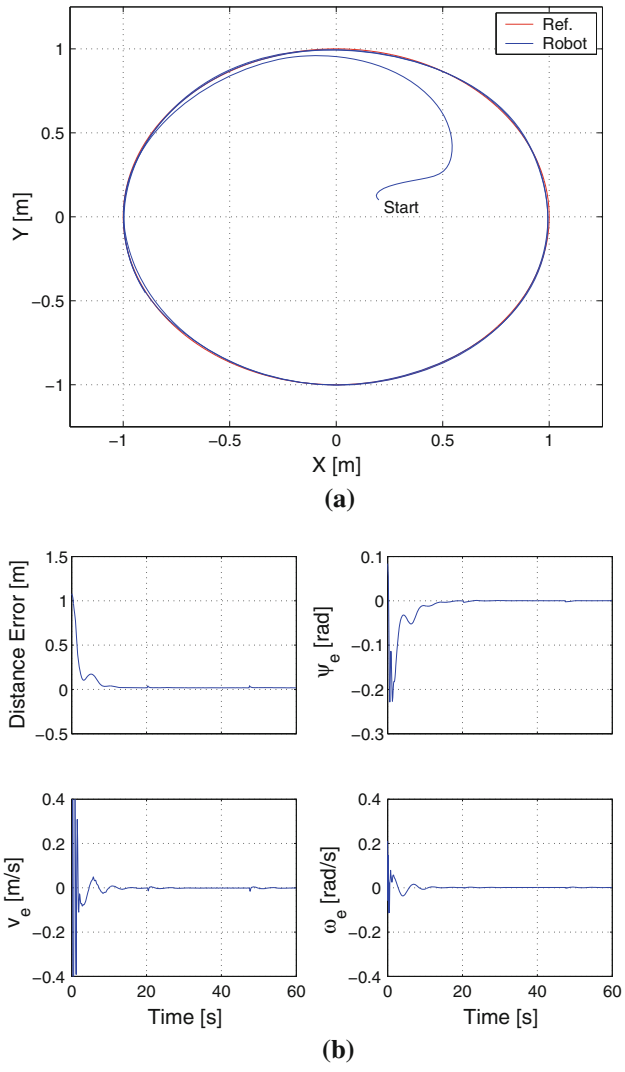

Fig. 9 Simulated case: disturbances included

updating law in (36), that is $\hat{\theta}_1 = 0.4042$, $\hat{\theta}_2 = 0.1877$, $\hat{\theta}_3 = -0.0069$, $\hat{\theta}_4 = 1.0261$, $\hat{\theta}_5 = 0.0405$, $\hat{\theta}_6 = 0.9239$, $\hat{\theta}_7 = -0.0304$ and $\hat{\theta}_8 = -0.1162$, causing structured uncertainties due to initial parameter errors. Unstructured uncertainties are simulated by adding white noise to the response velocities. Finally, variations up to 3.7 % of the nominal values of some real dynamic parameters emulate their variance along time [parameter identification and validation were performed in Cruz et al. (2011a)].

The kinematic and dynamic control laws given in (5) and (25), respectively, are cascaded, and the updating law (36) completes the system control, as illustrated in Fig. 2. Figure 9 presents a simulation result when the input disturbances are bounded to 1 cm/s and 0.02 rad/s. The dynamic controller gains are $k_v = 2$ and $k_\omega = 5$, the gains of the robustness term are $k_{rv} = 0.1$ and $k_{r\omega} = 0.1$, and the gain values associated with the parameter-updating law are $\Xi_i = 0.01$ and $\Gamma_i = 0.001$, with $i = 1 \ldots 8$. Moreover, the gains and saturation constants of the kinematic controller are set to the same values as in previous simulations, with $v_{\text{ref}}^{c} = 0.25\, m/s$.

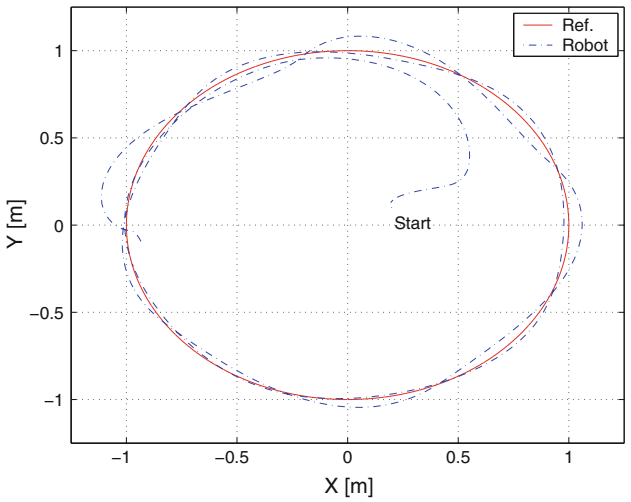

Fig. 10 Simulated case: disturbances included in a nonrobust control system

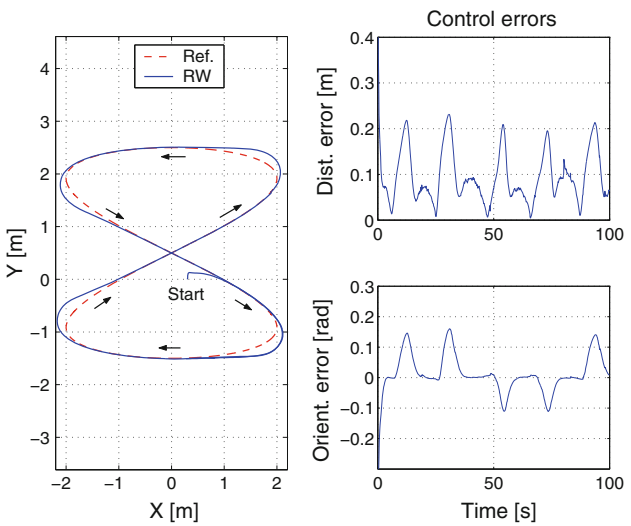

Fig. 11 Experiment: RW carrying a heavy person during path following

Figure 10 shows a simulation result when the robustness term is withdrawn from the dynamic controller, that is $k_{rv} = 0$ and $k_{r\omega} = 0$. One can see that the disturbances are able to degrade the system behavior when a robust control is not considered.

Experiments taking the complete system into account were performed with a RW carrying a heavy person (see Fig. 8), with the parameters of the wheelchair without any user taken as initial estimates. The voluntary was asked to move in the course of the experiment to introduce disturbances. Figure 11 shows the performance reached with all uncertainties and disturbances deliberately embedded. The corresponding excitation and response velocities are shown in Fig. 12, where it can be noticed that the measurement data (based only on the vehicle odometry) is very noisy.

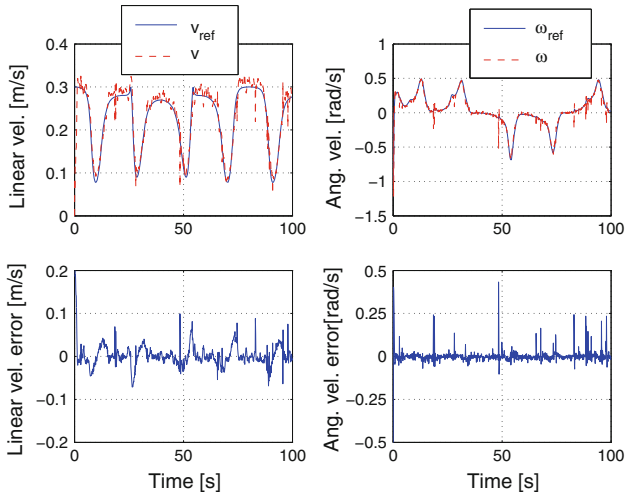

Fig. 12 Experiment: excitation and response velocities of the RW carrying a heavy person during path following

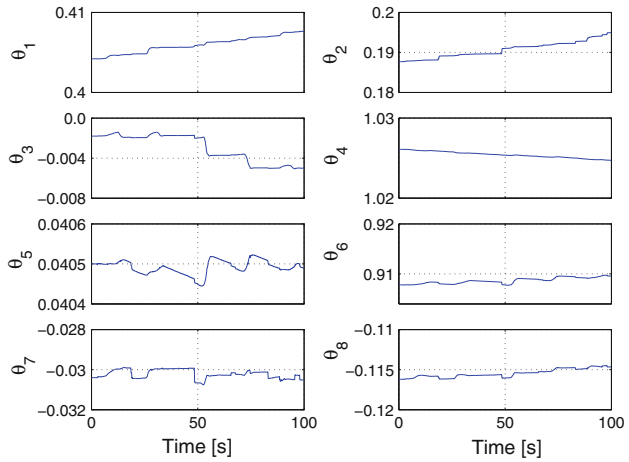

Fig. 13 Experiment: estimated parameters evolution for the RW carrying a heavy person

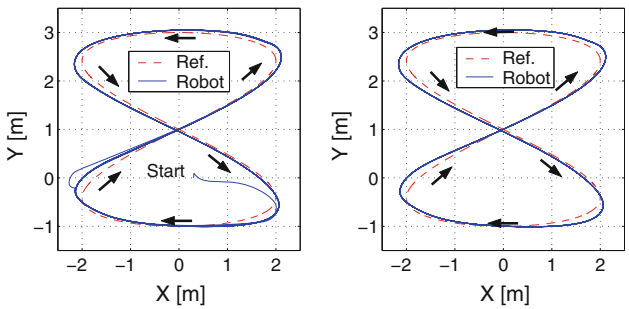

Fig. 14 Simulated case: a path with persistent excitation

The success of the control system in the presence of highly noisy measurement depends on a significant effort

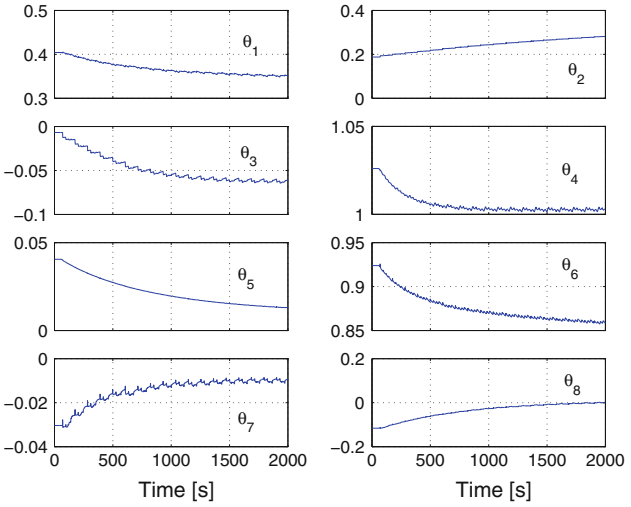

Fig. 15 Simulated case: evolution of the parameter estimates

during gain adjustment. A slow convergence of the estimate parameters is necessary to maintain system's stability, so that such convergence is not evident in Fig. 13. Hence, simulations for a long-term operation were performed. Figure 14 shows the vehicle behavior at the first (left side) and second (right side) half of the simulation time. It can be noticed a better performance in the last one, where the estimated parameters are close to their final values, as shown in Fig. 15.

6 Conclusion

A robust adaptive path-following control of a RW is designed here, and the closed-loop system stability is proved, when such controller is adopted. Such a control system is split into two parts, one taking care of the path-following kinematics and the other compensating for the vehicle dynamics. The first part assures that bounded command signals are sent to the vehicle, so that it converges to a reference path and follows it. The second one is responsible to reduce tracking errors due to the dynamic effects, which present structured and unstructured uncertainties as well as time-varying dynamics caused basically by the wheelchair user. Simulations and experiments on a RW with time-varying model parameters and different kinds of uncertainties embedded were performed, allowing us to verify that the controller presents a good performance.

Acknowledgments The authors thank CAPES (Brazil) and SPU (Argentina) for funding the partnership between Federal University of Espirito Santo/Brazil and National University of San Juan/Argentina (Project 018/04 CAPG-BA), and FAPES (Brazil) for financing part of this study (Process: 39385183/2007). Mr. Celeste also thanks CNPq, a Brazilian institution that supports scientific and technical development, for the scholarship he received for his Ph. D. research.

References

Aström, K. J., & Wittenmark, B. (2008). *Adaptive control* (2nd ed., Vol. 1). New York: Dover Publication.

Bessa, W. M., & BarrOto, R. S. S. (2010). Adaptive fuzzy sliding mode control of uncertain nonlinear systems. *SBA–Controle & Automação*, *21*(2), 117–126.

Coelho, P., & Nunes, U. (2005). Path-following control of mobile robots in presence of uncertainties. *IEEE Transactions on Robotics*, *21*(2), 252–261.

Cruz, C. D. L., & Carelli, R. (2006). Dynamic modeling and centralized formation control of mobile robots. In *32nd Annual conference of the IEEE industrial electronics society IECON* (pp. 3880–3885). Paris

Cruz, C. D. L., Carelli, R., & Bastos, T. F. (2011a). Adaptive control law for robotic wheelchairs. *IFAC–Control Engineering Practice*, *19*(2), 113–125.

Cruz, C. D. L., Celeste, W. C., & Bastos, T. F. (2011b). A robust navigation system for robotic wheelchairs. *IFAC–Control Engineering Practice*, *19*(6), 575–590.

de Wit, C. C., Siciliano, B., & Bastin, G. (1997). *Theory of robot control*. London: Springer-Verlag.

Ding, D., & Cooper, R. A. (2005). Electric-powered wheelchairs: A review of current technology and insight into the future directions. *IEEE Transactions on Neural Networks*, *1*(1), 22–34.

Do, K. D., Jiang, Z. P., & Pan, J. (2004). Simultaneous tracking and stabilization of mobile robots: An adaptive approach. *IEEE Transactions on Automatic Control*, *49*(7), 1147–1151.

dos Santos, F. P. N. (2011). Robotizatpo de uma cadeira de rodas. Master's thesis, Universidade Federal do Espírito Santo, Vitória. Brasil: ES.

Fierro, R., & Lewis, F. L. (1997). Control of a nonholonomic mobile robot: Backstepping kinematics into dynamics. *Journal of Robotics Systems*, *14*(3), 149–163.

Fioretti, S., Leo, T., & Longhi, S. (2000). A navigation system for increasing the autonomy and the security of powered wheelchairs. *IEEE Transactions on Rehabilitation Engineering*, *8*(4), 490–498.

Isidori, A. (1989). *Nonlinear control systems* (1st ed., Vol. 1). Berlin: Springer-Verlag.

Jordan M. A., & Bustamante J. L. (2008). A totally stable adaptive control for path tracking of time-varying autonomous underwater vehicles. *Proceedings of 17th IFAC World Congress*, *17*(1), 15985–15990.

Kim, C. H., Jung, J. H., & Kim, B. K. (2004). *Design of intelligent wheelchair for the motor disabled* (pp. 299–310). Daejeon: Proceedings of the Eighth International Conference on Rehabilitation Robotics.

Martins, F. N., Celeste, W. C., Carelli, R., Filho, M. S., & Filho, T. F. B. (2008). An adaptive dynamic controller for autonomous mobile robot trajectory tracking. *IFAC–Control Engineering Practice*, *16*(11), 1354–1363.

Parikh, S. P., Grassi, V., Kumar, V., & Okamoto, J. (2007). Integrating human inputs with autonomous behaviors on an intelligent wheelchair platform. *IEEE Transactions on Intelligent Systems*, *22*(2), 33–41.

Patre, P. M., MacKunis, W., Makkar, C., & Dixon, W. E. (2008). Asymptotic tracking for systems with structured and unstructured uncertainties. *IEEE Transactions on Control Systems Technology*, *16*(2), 373–379.

Sastry, S., & Bodson, M. (1989). *Adaptive control: Stability, convergence, and robustness* (Vol. 1). Portland, OR: Dover Publications.

Slotine, J.-J., & Li, W. (1988). Adaptive manipulator control: A case study. *IEEE Transactions on Automatic Control*, *33*(11), 995–1003.

Soetanto, D., Lapierre, L., & Pascoal, A. (2003). Adaptive, non-singular path-following control of dynamic wheeled robots. *Proceedings of the 42nd IEEE conference on decision and control*. Maui, Hawaii, USA.

Strang, G. (1988). *Linear algebra and its applications* (3rd ed., Vol. 1). New York: Thomson Learning, Inc.

Tanner, H. G., & Kyriakopoulos, K. J. (2003). Backstepping for non-smooth systems. *Automatica*, *39*(7), 1259–1265.

Vargas, J. A. R., & Hemerly, E. M. (2008). Observação adaptativa neural com convergência assintótica na presença de parâmetros variantes no tempo e distubios. *SBA–Controle & Automação*, *19*(1), 18–29.